

# RVLF: A Reinforcing Vision–Language Framework for Gloss-Free Sign Language Translation

Zhi Rao<sup>1</sup> Yucheng Zhou<sup>2</sup> Benjia Zhou<sup>3</sup> Yiqing Huang<sup>1</sup> Sergio Escalera<sup>4</sup> Jun Wan<sup>1\*</sup>

<sup>1</sup>Macau University of Science and Technology <sup>2</sup>SKL-IOTSC, CIS, University of Macau

<sup>3</sup>Beijing Institute of Technology, Zhuhai <sup>4</sup>University of Barcelona

zhir@student.must.edu.mo, yucheng.zhou@connect.um.edu.mo, jwan@must.edu.mo

## Abstract

Gloss-free sign language translation (SLT) is hindered by two key challenges: **inadequate sign representation** that fails to capture nuanced visual cues, and **sentence-level semantic misalignment** in current LLM-based methods, which limits translation quality. To address these issues, we propose a three-stage **reinforcing vision–language framework (RVLF)**. We build a large vision–language model (LVLM) specifically designed for sign language, and then combine it with reinforcement learning (RL) to adaptively enhance translation performance. First, for a sufficient representation of sign language, RVLF introduces an effective semantic representation learning mechanism that fuses skeleton-based motion cues with semantically rich visual features extracted via DINOv2, followed by instruction tuning to obtain a strong SLT-SFT baseline. Then, to improve sentence-level semantic misalignment, we introduce a GRPO-based optimization strategy that fine-tunes the SLT-SFT model with a reward function combining translation fidelity (BLEU) and sentence completeness (ROUGE), yielding the optimized model termed SLT-GRPO. Our conceptually simple framework yields substantial gains under the gloss-free SLT setting without pre-training on any external large-scale sign language datasets, improving BLEU-4 scores by +5.1, +1.11, +1.4, and +1.61 on the CSL-Daily, PHOENIX-2014T, How2Sign, and OpenASL datasets, respectively. To the best of our knowledge, this is the first work to incorporate GRPO into SLT. Extensive experiments and ablation studies validate the effectiveness of GRPO-based optimization in enhancing both translation quality and semantic consistency.

## 1. Introduction

Sign language translation (SLT) aims to bridge the communication gap between the deaf and hearing communities by translating sign/gesture videos [43, 44, 55] into spoken language text [4, 54]. Traditional gloss-based methods decompose SLT into two stages: sign-to-gloss and gloss-to-text [5–7, 57]. Although glosses provide linguistic structure, they are inherently limited by high annotation costs, cross-linguistic inconsistencies, and annotation noise, hindering scalability for real-world deployment [5]. With the rapid advancement of LLMs and VLM pre-training, gloss-free SLT has gained increasing attention as a more scalable and linguistically flexible alternative to gloss-based systems [8, 9, 16, 22, 24, 45, 45, 54]. These approaches aim to directly map sign videos to spoken text, eliminating the dependency on costly gloss annotations. However, despite the expressive power of LLMs, current gloss-free methods still struggle to achieve accurate and fluent translations. We identify two core obstacles underlying this limitation. The first concerns the **inadequate sign representation**. Existing models [8, 9, 16, 22, 24, 45, 48, 54] often rely on global image and/or skeleton-level features<sup>1</sup>, as shown in Fig. 1 (a). However, accurate sign semantics is based on multiple cues, facial expressions, lip movements, hand gestures, and motion trajectories [1, 12, 15, 17, 41, 56]. Yet most gloss-free SLT models lack representations tailored to these characteristics. Without considering such cues, the extracted features fail to capture sufficient sign-specific semantics. The second obstacle lies in the **sentence-level semantic misalignment**. Previous models [8, 9, 16, 22, 45, 48, 54] typically enhance sign representations through vision–language pre-training, and subsequently fine-tune an LLM using a cross-entropy (CE) objective that optimizes token-level likelihoods, as shown in Fig. 1 (a). However, such token-wise optimization merely enforces local lexical accuracy with-

\*Corresponding author

<sup>1</sup>Uni-Sign introduces hand RGB images only as compensation when skeleton confidence is low, but its primary input remains skeletons.

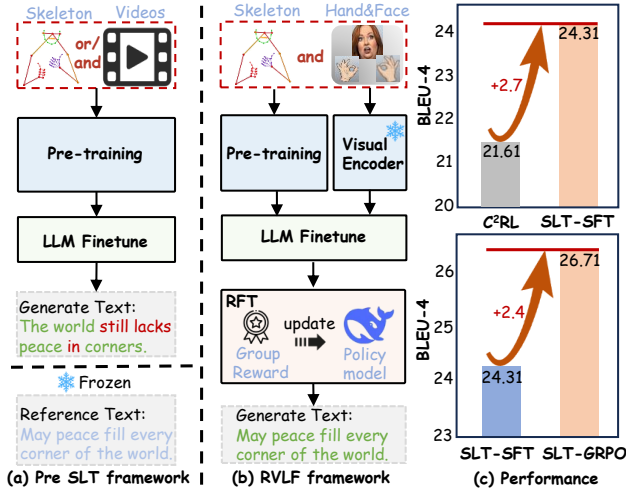


Figure 1. The overview illustrates the difference between previous gloss-free SLT frameworks (a) and the proposed RVLF framework (b), along with the performance of our method on the CSL-Daily [57] dataset (c). *REF*: Reinforcement Fine-Tuning.

out directly constraining the fidelity or completeness of the generated sentences. As a result, the model lacks explicit guidance to produce translations that are semantically aligned and coherent with the reference text. To overcome the first limitation, an effective sign semantic representation is developed. Unlike relevant works [15, 17, 24, 56], the proposed approach performs cross-lingual visual–language pre-training on the skeleton encoder, using text as supervision to learn high-quality global representations of sign language cues, including motion trajectories, hand gestures, and lip movements. The resulting global representations are further fused with fine-grained hand and facial features extracted by DINOv2 [32], enabling complementary modeling of facial expressions and enhanced representation of hand gestures, as shown in Fig. 1 (b). Following the standard LVLMs training paradigm [11, 28, 29, 51], we introduce a lightweight projector to map the fused sign visual features into the text embedding space of the LLM and conduct instruction tuning with LoRA to adapt the LLM for generating translation text. In this way, we achieve an SFT paradigm specifically tailored to the characteristics of sign language and obtain strong translation performance. We name this model SLT-SFT. As shown in Fig. 1 (c), our SLT-SFT improves BLEU-4 by 2.7 compared to the current State-of-the-Art (SOTA) model C<sup>2</sup>RL [9] under the setting without pre-training on any external large-scale sign language datasets. To address the second limitation, we introduce Group Relative Policy Optimization (GRPO) [38] for the first time in the SLT domain and use it as a sentence-level reinforcement optimization strategy, forming our SLT-GRPO model as shown in Fig. 1 (b). Unlike standard supervised fine-tuning, reinforcement optimization enables the model to learn from its own generated translations by com-

paring them with reference sentences to compute sentence-level rewards that guide subsequent policy updates. In this framework, the translation process is formulated as a policy generation procedure, where rewards are derived from sentence-level metrics that evaluate the semantic and structural alignment between generated and reference sentences. These metrics capture N-gram overlap and semantic coverage, encouraging the model to generate semantically equivalent outputs rather than merely high-probability tokens. Meanwhile, GRPO computes relative rewards within each group to stabilize optimization, reduce variance, and improve training efficiency. Overall, this method aligns the training objective with the evaluation metrics, leading to significant improvements in semantic consistency and translation accuracy. As shown in Fig. 1 (c), SLT-GRPO improves BLEU-4 by 2.4 compared to the SLT-SFT model.

Our main contributions are summarized as follows:

- We propose a three-stage RVLF: (1) Pre-training: visual–language pre-training using skeleton-based input; (2) SFT: fine-tuning the LLM using sufficient sign representations; (3) RFT: sentence-level optimization using the GRPO strategy.
- We introduce an effective and semantically expressive representation of sign language and fine-tune an LLM with strong linguistic capabilities to achieve high-quality sign language translation, referred to as SLT-SFT.
- To address the sentence-level semantic misalignment in SLT, we apply GRPO-based reinforcement optimization with sentence-level rewards, forming SLT-GRPO.
- RVLF achieves state-of-the-art results on multiple datasets and even surpasses Uni-Sign pre-trained on a large-scale external sign language dataset on CSL-Daily.

## 2. Related Work

### 2.1. Sign Language Translation

Sign Language Translation (SLT) aims to convert sign videos into spoken language sentences, posing unique challenges due to the spatiotemporal complexity of gestures and syntactic divergence from spoken language. Existing methods are broadly categorized into gloss-based and gloss-free approaches. Gloss-based methods leverage intermediate gloss annotations that provide structured, monotonic alignments between visual input and linguistic units, often incorporating auxiliary Sign Language Recognition (SLR) modules or directly decoding gloss sequences [5–7, 57]. However, gloss annotations are costly to obtain and limit scalability. To overcome this, gloss-free SLT seeks to directly map sign videos to spoken language without gloss supervision. Early studies [3, 5, 23, 48, 52] demonstrated its feasibility, though a performance gap remains relative to gloss-based systems. Recent efforts employ visual–language pre-training to enhance representation learning. GFSLT [54],

for example, adapts CLIP [35] for sign language, inspiring follow-up work [8, 16, 45]. Other models [9, 22] leverage fine-grained alignment between sign segments and text, achieving competitive results. In parallel, large-scale pre-training on extensive sign corpora [24, 37, 42] has shown promise but comes at high computational and annotation costs. In contrast, our work focuses on exploring more comprehensive and semantically expressive representations of sign language at the algorithmic level, and leverages large language models with strong linguistic understanding and generation capabilities to decode such representations, thereby advancing the progress of gloss-free SLT.

## 2.2. Reasoning Large Vision-Language Models

Recent advances in Large Vision–Language Models (LVLMs) have greatly improved cross-modal understanding and generation. Early frameworks such as LLaVA [28] introduced multimodal instruction tuning for large language models, substantially enhancing visual reasoning and alignment. The Qwen2.5-VL [2] and Qwen3-VL [34] series further expanded these capabilities by incorporating dynamic resolution and temporal modeling, achieving stronger multilingual comprehension and fine-grained video understanding. Recently, reinforcement learning (RL) has been shown to further enhance reasoning in large models. OpenAI o1 [20] demonstrated that outcome-based RL significantly improves the reasoning ability of LLMs, while DeepSeek-R1 [18] adopted rule-based rewards with the GRPO algorithm to teach structured reasoning. Building upon this, several works such as R1-OneVision [47], VisualThinker-R1-Zero [58], and VisionR1 [19] have extended the R1 paradigm to multimodal settings, constructing step-by-step reasoning datasets and refining reinforcement fine-tuning strategies. Inspired by these reasoning-enhanced LVLM paradigms, we introduce the RVLf for sign language translation, which integrates instruction tuning and GRPO-based reinforcement optimization to enhance semantic alignment.

## 3. Method

In this paper, we propose a three-stage training framework for sign language translation (Fig. 2). **Stage 1** (Sec. 3.1): We perform visual-language pre-training, aligning skeleton features with textual representations through combined contrastive and translation objectives. **Stage 2** (Sec. 3.2): We integrate the pre-trained skeleton features with semantically enriched hand–face features extracted by DINOv2 [32], and fine-tune an LLM via instruction tuning to generate translations. **Stage 3** (Sec. 3.3): We apply GRPO optimization [38], using sentence-level metrics as rewards to further refine translation quality.

### 3.1. Vision-Language Pre-training

The goal of this stage is to learn robust multimodal representations by aligning sign language videos with their corresponding textual translations. Our pre-training framework is driven by two core objectives: a contrastive alignment objective and a translation objective.

**Contrastive Alignment.** To establish a fine-grained alignment between visual and textual modalities, we introduce a contrastive learning objective. This requires encoding sign videos and text into comparable semantic spaces.

*Skeleton Encoder.* To capture the intricate dynamics of sign language, the Skeleton Encoder (SkeletonEnc) transforms a given sign video  $V$  into a sequence of visual representations. First, we employ MMPose [13] to extract 2D keypoints for the upper body, face, and hands from each frame, converting the video  $V$  into a skeleton sequence  $S$ . This sequence is then processed by CoSign [21], a GCN-based model that handles different sign groups (body, hands, face) independently to learn their unique co-occurrence patterns. The encoder thus yields a sequence of skeleton features:

$$Z_s = \text{SkeletonEnc}(V) = \{z_{s,1}, \dots, z_{s,m}\}, \quad (1)$$

where  $m$  is the number of frames in the video.

*Text Encoder.* The corresponding text  $T$  is processed by the Text Encoder (TextEnc), which is derived from the initial layers of the mBART [30] encoder. This produces a sequence of semantic text embeddings:

$$Z_t = \text{TextEnc}(T) = \{z_{t,1}, \dots, z_{t,l}\}, \quad (2)$$

where  $l$  is the number of tokens in the text.

*InfoNCE Loss.* Given a mini-batch of  $B$  video-text pairs, the skeleton features  $Z_s$  and text features  $Z_t$  are padded to lengths  $M$  and  $L$ , respectively. Both sequences are then projected into a  $D$ -dimensional embedding space by separate MLPs, resulting in  $F_S \in \mathbb{R}^{M \times D}$  and  $F_T \in \mathbb{R}^{L \times D}$ . Let  $f_i$  and  $t_j$  be the L2-normalized row vectors of  $F_S$  and  $F_T$ . The cross-modal similarity matrix  $E \in \mathbb{R}^{M \times L}$  is then computed as:

$$E_{i,j} = f_i \cdot t_j^\top. \quad (3)$$

To calculate the global sign-skeleton-to-text similarity  $z_{S,T}$ , a row-wise Softmax [10] is applied to  $E$  to obtain the attention weights  $P$ :

$$P_{i,j} = \frac{\exp(E_{i,j}/\tau)}{\sum_{k=1}^L \exp(E_{i,k}/\tau)}, \quad (4)$$

where  $\tau$  denotes a trainable temperature parameter. A re-weighted similarity is then computed for each skeleton segment:

$$e_{S \rightarrow T,i} = \sum_{j=1}^L (P_{i,j} \times E_{i,j}). \quad (5)$$

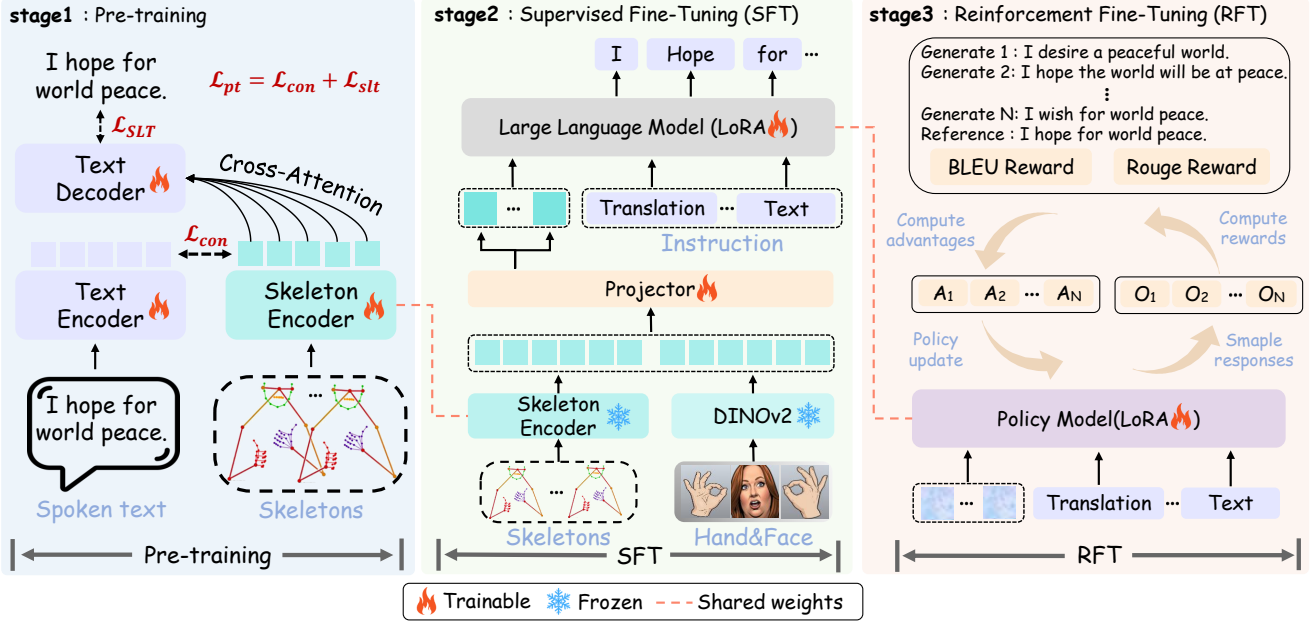


Figure 2. The framework of RVLF. **Stage 1 (Pre-training)**: A vision-language foundation is built using contrastive ( $\mathcal{L}_{con}$ ) and translation ( $\mathcal{L}_{slT}$ ) losses. **Stage 2 (Supervised Fine-Tuning)**: Adequate sign language representations are used as visual inputs, while appropriate instruction tuning is applied to the large language model to construct a vision-language model specifically tailored for sign language understanding and translation. **Stage 3 (Reinforcement Fine-Tuning)**: A GRPO-based optimization strategy is employed to further fine-tune the policy model from the previous stage using a reward function based on sentence-level translation metrics, improving the overall translation performance.

Finally, the global similarity is computed by averaging over all skeleton segments:

$$z_{S,T} = \frac{1}{M} \sum_{i=1}^M e_{S \rightarrow T, i}. \quad (6)$$

Symmetrically, the global text-to-sign-skeleton similarity  $z_{T,S}$  is computed. To apply contrastive learning across the batch, we compute these global similarity scores for every skeleton sequence  $S^{(b)}$  and every text sequence  $T^{(b')}$  in the mini-batch (where  $b, b' \in \{1, \dots, B\}$ ). This populates two matrices,  $Z_{S2T}, Z_{T2S} \in \mathbb{R}^{B \times B}$ , where the element  $Z_{S2T}^{(b,b')} = z_{S^{(b)}, T^{(b)'}}$  represents the similarity from the  $b$ -th skeleton to the  $b'$ -th text. A bidirectional InfoNCE loss is then applied to these matrices:

$$\mathcal{L}_{S2T} = -\frac{1}{B} \sum_{b=1}^B \log \frac{\exp(Z_{S2T}^{(b,b)}/\tau')}{\sum_{b'=1}^B \exp(Z_{S2T}^{(b,b')}/\tau')}, \quad (7)$$

$$\mathcal{L}_{T2S} = -\frac{1}{B} \sum_{b=1}^B \log \frac{\exp(Z_{T2S}^{(b,b)}/\tau')}{\sum_{b'=1}^B \exp(Z_{T2S}^{(b,b')}/\tau')}, \quad (8)$$

$$\mathcal{L}_{con} = \beta \mathcal{L}_{S2T} + (1 - \beta) \mathcal{L}_{T2S}, \quad (9)$$

where  $\tau'$  is a temperature parameter and  $\beta$  balances the two directional losses.

**Translation Objective.** To equip the model with generative capabilities, we employ a translation objective. The skeleton representations  $Z_s$  are fed into a Text Decoder, which is adapted from the mBART decoder, to generate a textual translation. This is optimized via a standard cross-entropy loss, similar to a captioning task [49]:

$$\mathcal{L}_{slT} = -\sum_{i=1}^L \log P(y_i | y_{<i}, Z_s), \quad (10)$$

where  $y_i$  is the  $i$ -th token in the ground-truth sentence and  $L$  is the padded sequence length.

**Pre-training Objective.** The final pre-training objective combines the contrastive and translation losses to learn representations that are both well-aligned and generative:

$$\mathcal{L}_{pt} = \mathcal{L}_{con} + \mathcal{L}_{slT}. \quad (11)$$

### 3.2. Supervised Fine-Tuning

In the second stage, we fine-tune the LLM using the learned sign representations. In addition to the skeleton embeddings, we incorporate dense visual cues extracted by DINOv2 [32]. It is motivated by the observation that the sparse skeletal modality alone is insufficient to capture the full expressiveness of sign language, as crucial semantic cues often lie in fine-grained hand shapes and facial expressions.

**Dense Visual Cue Extraction.** To capture fine-grained motion and expression details, we extract dense visual cues from hand and face regions. Specifically, we first detect bounding boxes for the hands and face in each video frame, then crop these regions and feed them into a pre-trained DINOv2 [32] model to obtain semantically rich feature sequences. To align feature dimensions for fusion, the extracted features are linearly projected to match the skeleton representation. The fused enhanced representation is computed as:

$$Z_e = Z_s + \alpha \cdot Z_{face} + \beta \cdot Z_{hand} \quad (12)$$

where  $\alpha$  and  $\beta$  are tunable coefficients controlling the relative contributions of facial and hand cues. Finally, the enhanced embedding is projected into the target latent space via a learnable MLP transformation:

$$Z = \text{MLP}(Z_e). \quad (13)$$

**LLM Fine-Tuning.** We employ Qwen3 [46] model as the base large language model (LLM) for sign language translation. The aligned sign features  $Z$  are prepended to the LLM’s input embeddings. The model is then fine-tuned using LoRA-based instruction tuning to autoregressively generate the target textual sequence, written as:

$$\mathcal{L}_{\text{sft}} = - \sum_{t=1}^L \log p_{\theta}(y_t | y_{<i}, Z), \quad (14)$$

where  $\theta$  denotes the trainable LoRA parameters in the LLM.

### 3.3. Reinforcement Fine-Tuning

SFT optimizes models at the token level via cross-entropy, thereby overlooking sentence-level qualities such as semantic fidelity and completeness. To align training with these holistic objectives, a reinforcement fine-tuning stage using the GRPO is introduced.

The GRPO algorithm begins by sampling  $N$  candidate outputs  $\{O_1, \dots, O_N\}$  from the current policy  $\pi_{\theta}$  for a given query prompt  $q$ . Each response  $O_i$  is then evaluated by a reward function  $R(q, O_i)$  to obtain a raw reward score  $r_i$ . In our SLT task, the prompt  $q$  corresponds to the fused sign features  $Z_{\text{sign}}$ , and the candidate outputs  $\{O_1, \dots, O_N\}$  are the translations generated by the policy. The reward function  $R(q, O_i)$  is designed to measure the quality of a generated translation  $O_i$  against the ground-truth reference sentence  $T$ . It is computed as a combination of BLEU-4 and ROUGE-L scores, which capture N-gram overlap and semantic coverage, respectively:

$$R(q, O_i) = \lambda \text{BLEU-4}(O_i, T) + (1 - \lambda) \text{ROUGE}(O_i, T) \quad (15)$$

This reward directly incentivizes the model to generate outputs that are semantically and structurally superior at the sentence level.

To measure the relative quality of each response within the sampled group, GRPO standardizes the raw rewards to obtain the advantage value in Eq. 16. The advantage value  $A_i$  denotes the normalized advantage of the response  $O_i$  relative to other samples within the group.

$$A_i = \frac{r_i - \text{mean}\{r_1, r_2, \dots, r_N\}}{\text{std}\{r_1, r_2, \dots, r_N\}} \quad (16)$$

The policy  $\pi_{\theta}$  is updated with a training objective (Eq. 17), designed to encourage the generation of responses with higher advantages.

$$\mathcal{J}_{\text{GRPO}}(\theta) = \mathbb{E}_{\{O_i\}_{i=1}^N \sim \pi_{\text{old}}(\cdot|q)} \left[ \frac{1}{N} \sum_{i=1}^N L_{\text{GRPO}}^{(i)} \right] \quad (17)$$

$$L_{\text{GRPO}}^{(i)} = \min(c_1 \cdot A_i, c_2 \cdot A_i) - \beta D_{\text{KL}}(\pi_{\theta} \| \pi_{\text{ref}}) \quad (18)$$

$$c_1 = \frac{\pi_{\theta}(O_i | q)}{\pi_{\text{old}}(O_i | q)}, c_2 = \text{clip} \left( \frac{\pi_{\theta}(O_i | q)}{\pi_{\text{old}}(O_i | q)}, 1 - \varepsilon, 1 + \varepsilon \right) \quad (19)$$

where  $D_{\text{KL}}(\pi_{\theta} \| \pi_{\text{ref}})$  denotes the KL divergence between the current policy  $\pi_{\theta}$  and the reference policy  $\pi_{\text{ref}}$ , which serves as a regularization term to prevent large deviations. The clipping mechanism in  $c_2$  stabilizes training by constraining the policy update ratio.

## 4. Experiment

### 4.1. Experimental Setup

**Datasets.** We evaluated our method on four main-stream sign language datasets: CSL-Daily[57], PHOENIX-2014T[4], How2Sign[14] and OpenASL[39]. PHOENIX-2014T is a benchmark dataset for German Sign Language to spoken German translation. It is collected from German weather broadcast programs. The CSL-Daily dataset is a Chinese sign language (CSL) dataset recorded in the laboratory whose topic focuses on daily life. How2Sign is a large-scale American Sign Language (ASL) dataset comprising approximately 80 hours of sign language videos. Collected from instructional videos across diverse categories, the dataset represents a more open-domain setting. The OpenASL dataset is an ASL dataset collected from online videos that cover various topics.

**Evaluation Metrics.** We evaluate translation performance using standard metrics commonly employed in sign language translation, including BLEU and ROUGE-L scores. BLEU evaluates **translation fidelity** by measuring the overlap of n-grams between the model output and the reference translation [33], reflecting how well the generated text preserves the original meaning. In contrast, ROUGE-L assesses **sentence completeness** by calculating the length of the longest common subsequence between the generated and reference texts [26], indicating the overall structural and semantic coverage of the translation.

Method	ROUGE	B@1	B@2	B@3	B@4
<i>Gloss-based</i>					
SLRT <sup>†</sup> [5]	36.74	37.38	24.36	16.55	11.79
SignBT [57]	49.31	51.42	37.26	27.76	21.34
MMTLB [6]	53.25	53.31	40.41	30.87	23.92
SLTUNET [50]	54.08	54.98	41.44	31.84	25.01
TS-SLT [7]	<u>55.72</u>	<u>55.44</u>	<u>42.59</u>	<u>32.87</u>	<u>25.79</u>
CV-SLT [53]	<b>57.06</b>	<b>58.29</b>	<b>45.15</b>	<b>35.77</b>	<b>28.94</b>
<i>Gloss-free</i>					
Uni-Sign [24]	56.51	55.08	42.14	32.98	26.36
TSPNet* [23]	18.38	17.09	8.98	5.07	2.97
GASLT [48]	20.35	19.90	9.94	5.98	4.07
NSLT <sup>†</sup> [3]	34.54	34.16	19.57	11.84	7.56
GFSLT-VLP [54]	36.44	39.37	24.93	16.26	11.00
Sign2GPT [45]	42.36	41.75	28.73	20.60	15.40
SignLLM [16]	39.91	39.55	28.13	20.07	15.75
VAP [22]	48.56	49.99	-	-	20.85
C <sup>2</sup> RL [9]	48.21	49.32	36.28	27.54	21.61
SLT-SFT(Ours)	<u>52.43</u>	<u>52.34</u>	<u>39.03</u>	<u>30.32</u>	<u>24.31</u>
SLT-GRPO(Ours)	<b>55.92</b>	<b>54.96</b>	<b>42.45</b>	<b>33.33</b>	<b>26.71</b>

Table 1. SLT results on CSL-Daily dataset. \* denotes methods reproduced by [48]. † denotes methods reproduced by [57]. The result of the work trained on large-scale external sign language dataset (CSL-News [24]) is shown in gray. The best scores are **bolded**. The second-best scores are underlined.

**Implementation details.** We use CoSign [21] and a three-layer Transformer encoder as our skeleton encoder. The text encoder and decoder use the fully transformer blocks, which consist of three layers each in both the encoder and decoder. Each layer includes 8 attention heads, a hidden size of 512, and a feed-forward dimension of 2048. The transformer encoder of skeleton encoder shares the same configuration as the text encoder but utilizes only the encoder component. Unlike previous work [28], we conduct experiments on four different sign language datasets in Chinese, German, and American, using a unified decoder-only large language model (Qwen3). All experiments are conducted on four NVIDIA V100 GPUs (32GB) in float16 precision to optimize memory efficiency. During pre-training, we employ the SGD [36] optimizer with a learning rate of 0.01 and a weight decay of 0.001. During supervised fine-tuning, we employed the AdamW optimizer [31]. The LLM was trained with a learning rate of  $2 \times 10^{-4}$ , while the multimodal projector used a learning rate of  $2 \times 10^{-5}$ . The weight decay was set to 0. During reinforcement fine-tuning, we employed the AdamW optimizer [31]. Trained with a learning rate of  $2 \times 10^{-5}$ . The three stages are trained for 200, 40, and 2 epochs, respectively. For each stage, the model achieving the highest BLEU-4 score on the validation set is selected as the final model.  $\alpha$ ,  $\beta$ , and  $\lambda$  are set as 1, 1, and 0.5, respectively. More implementation details are provided in the supplementary material.

Method	ROUGE	B@1	B@2	B@3	B@4
<i>Gloss-based</i>					
SLRT [5]	-	46.61	33.73	26.19	21.32
SignBT [57]	49.54	50.80	37.75	29.72	24.32
TS-SLT [7]	53.48	<b>54.90</b>	<u>42.43</u>	<u>34.46</u>	<u>28.95</u>
CV-SLT [53]	<b>54.33</b>	<u>54.88</u>	<b>42.68</b>	<b>34.79</b>	<b>29.27</b>
<i>Gloss-free</i>					
NSLT [3]	31.80	32.24	19.03	12.83	9.58
SLRT-GF* [5]	31.10	30.88	18.57	13.12	10.19
TSPNet [23]	34.96	36.10	23.12	16.88	13.41
CSGCR [52]	38.85	36.71	25.40	18.86	15.18
GASLT [48]	39.86	39.07	26.74	21.86	15.74
GFSLT-VLP [54]	42.49	43.71	33.18	26.11	21.44
Sign2GPT [45]	48.90	49.54	35.96	28.83	22.52
FLa-LLM [8]	45.27	46.29	35.33	28.03	23.09
Sign-llm [16]	44.49	45.21	34.78	28.05	23.40
LLaVA-SLT [25]	50.44	51.20	37.51	29.39	23.42
VAP [22]	51.28	53.07	-	-	26.16
C <sup>2</sup> RL [9]	50.96	52.81	40.20	32.20	26.75
SLT-SFT(Ours)	<u>51.81</u>	<u>53.29</u>	<u>40.44</u>	<u>32.35</u>	<u>26.83</u>
SLT-GRPO(Ours)	<b>52.56</b>	<b>53.60</b>	<b>41.20</b>	<b>33.24</b>	<b>27.86</b>

Table 2. Experimental results on PHOENIX14T dataset. No prior work has been pre-trained on large-scale external sign language datasets and evaluated on the PHOENIX-2014T dataset.

## 4.2. Main Results

**Experiment on CSL-Daily Datasets.** Table 1 summarizes the comparison with previous SLT models. In the gloss-free setting for fair comparison, our SLT-SFT achieves strong gains over all methods that do not use large-scale external sign-language pre-training, outperforming the previous SOTA C<sup>2</sup>RL [9] by a clear margin (24.31 vs. 21.61 in BLEU-4). Despite this progress, a gap remains to Uni-Sign [24] (26.36), which benefits heavily from costly large-scale pre-training. Furthermore, our sentence-level optimization further enforces translation fidelity, enabling SLT-GRPO to boost BLEU-4 by +2.4 and surpass Uni-Sign (26.71 vs. 26.36). SLT-GRPO also substantially outperforms C<sup>2</sup>RL [9] (+5.1). Moreover, SLT-GRPO shows competitive or superior performance to several gloss-based methods, outperforming SignBT (26.71 vs. 21.34) and TS-SLT (26.71 vs. 25.79), and approaching the gloss-based SOTA CV-SLT (26.71 vs. 28.94). These results collectively highlight the advantages and efficiency of our method across gloss-free and gloss-based settings.

**Experiment on PHOENIX14T Dataset.** As shown in Table 2, SLT-SFT slightly surpasses the previous SOTA C<sup>2</sup>RL (26.83 vs. 26.75) in the gloss-free setting. And the proposed sentence-level optimization further improves performance: SLT-GRPO reaches 27.86 BLEU-4, establishing a new gloss-free SOTA (+1.11 over C<sup>2</sup>RL). Despite using no gloss supervision, SLT-GRPO outperforms early gloss-based models (SLRT 21.32; SignBT 24.32) and narrows the gap to the gloss-based SOTA CV-SLT (29.27).

Method	ROUGE	B@1	B@2	B@3	B@4
YouTube-ASL [42]	-	37.8	24.1	16.9	12.4
SignMusketeers [17]	-	41.5	27.2	19.3	14.3
Uni-Sign [24]	36.0	40.2	27.1	19.7	14.9
SSVP-SLT [37]	38.4	43.2	28.8	20.8	15.5
YouTube-ASL [42]	-	15.0	5.1	2.3	1.2
GloFE-VN [27]	12.6	14.9	7.3	3.9	2.2
SSVP-SLT [37]	25.7	30.2	16.7	10.5	7.0
OpenSLT [40]	-	34.0	19.3	12.2	8.0
C <sup>2</sup> RL [9]	27.0	29.1	18.6	12.9	9.4
FLa-LLM [8]	27.8	29.8	19.0	13.3	9.7
VAP [22]	27.8	<u>39.2</u>	-	-	<u>12.9</u>
SLT-SFT (Ours)	<u>31.3</u>	38.3	<u>23.7</u>	<u>16.5</u>	12.2
SLT-GRPO (Ours)	<b>34.7</b>	<b>39.4</b>	<b>25.3</b>	<b>18.6</b>	<b>14.3</b>

Table 3. Experimental results on the How2Sign dataset. The results of models pre-trained on a large-scale external sign language dataset (Youtube-ASL [42]) are shown in gray.

Method	ROUGE	B@1	B@2	B@3	B@4
Uni-Sign [24]	43.22	49.35	36.22	28.55	23.14
Conv-GRU <sup>†</sup> [3]	16.10	16.11	8.85	6.18	4.58
I3D-transformer [39]	18.64	18.31	10.15	7.19	5.66
OpenASL [39]	21.02	20.92	12.08	8.59	6.72
GloFE-VN [27]	21.75	21.56	12.74	9.05	7.06
C <sup>2</sup> RL [9]	31.36	31.46	21.85	16.58	13.21
VAP [22]	41.38	45.92	-	-	21.23
SLT-SFT (Ours)	<u>41.84</u>	<u>46.03</u>	<u>33.64</u>	<u>26.31</u>	<u>21.28</u>
SLT-GRPO (Ours)	<b>43.92</b>	<b>48.73</b>	<b>35.40</b>	<b>27.99</b>	<b>22.84</b>

Table 4. Experimental results on OpenASL dataset. The result of the work trained on a large-scale external sign language dataset (Youtube-ASL [42]) is shown in gray.

**Experiment on How2Sign Dataset.** As shown in Table 3, SLT-SFT attains a slightly lower BLEU-4 than VAP (12.2 vs. 12.9) but achieves a higher ROUGE (31.3 vs. 27.8), indicating stronger semantic completeness. SLT-GRPO further lifts BLEU-4 to 14.3, establishing a new gloss-free SOTA (+1.4 over VAP). Despite using no large-scale sign-language pre-training, SLT-GRPO surpasses Youtube-ASL, performs comparably to SignMusketeers, and approaches Uni-Sign and SSVP-SLT (14.9 and 15.5).

**Experiment on OpenASL Dataset.** Table 4 reports results on OpenASL, which, like How2Sign, lacks gloss annotations; all comparisons are gloss-free. SLT-SFT slightly outperforms the previous SOTA VAP (21.28 vs. 21.23), and SLT-GRPO further improves performance to 22.84, setting a new SOTA (+1.61 over VAP). Despite the absence of large-scale external pre-training, SLT-GRPO remains competitive with Uni-Sign (22.84 vs. 23.14).

### 4.3. Ablation Study.

To further investigate the effectiveness of each component of the proposed RVLf method, we conduct extensive ablation experiments on the CSL-Daily dataset.

Setting	ROUGE	B@1	B@2	B@3	B@4
SLT-GRPO	55.92	54.96	42.45	33.33	26.71
w/o Pre-training	42.10	41.68	29.68	22.20	17.22
w/o DINOv2	51.45	49.51	37.66	28.10	22.93
w/o RFT	53.81	52.34	39.03	30.32	24.31

Table 5. Comparison of evaluation metrics across different settings. *w/o Pre-training*: SLT-SFT model trained with skeleton features without pre-training; *w/o DINOv2*: SLT-SFT model trained without hand or facial features extracted by DINOv2; *w/o RFT*: Equivalent to the SLT-SFT model.

Face	Hand	ROUGE	B@1	B@2	B@3	B@4
×	×	51.45	49.51	37.66	28.10	22.93
✓	×	52.84	52.12	38.73	29.86	23.69
×	✓	52.74	51.32	38.10	29.35	23.27
✓	✓	53.81	52.34	39.03	30.32	24.31

Table 6. Comparison of SLT-SFT model performance under various DINOv2 features. ✓ represents the use of the corresponding input feature.

**Ablation on the framework.** Table 5 presents an ablation study across different framework settings. Removing the pre-training stage results in a significant performance drop (-7.09 BLEU@4), highlighting the domain gap between sign language videos and general video data, and underscoring the need for a specialized skeleton encoder to learn high-quality representations of sign language cues. Text-supervised training effectively guides the encoder toward more discriminative semantic representations. Removing the fine-grained sign semantics from DINOv2 leads to a -1.38 BLEU@4 drop, demonstrating the value of hand and facial features in capturing sign-relevant information. These features contribute to complementary modeling of facial expressions and enhanced representation of hand gestures. Finally, removing the RFT stage causes a -2.40 BLEU@4 drop, indicating that sentence-level reinforcement optimization improves semantic consistency and translation accuracy by encouraging the model to consider sentence fidelity rather than just high-probability tokens.

**Ablation on DINOv2 features.** As shown in Table 6, adding either hand or face features extracted by DINOv2 results in varying degrees of performance improvement, indicating that both types of features provide complementary semantic cues to the sign representations. Notably, incorporating face features yields larger gains, likely because facial expressions offer more informative cues for enriching the global representations learned by the skeleton encoder. Moreover, combining both hand and face features achieves even greater improvements than using either alone, highlighting the strong complementarity between these two forms of fine-grained sign semantics.

BLEU-4	ROUGE	ROUGE	B@1	B@2	B@3	B@4
✓	×	55.26	55.26	41.97	32.78	26.23
×	✓	55.03	54.17	41.48	32.20	25.66
✓	✓	55.92	54.96	42.45	33.33	26.71

Table 7. Comparison of evaluation metrics under different reward configurations. ✓ denotes the use of the corresponding reward function.



Figure 3. Learning curves of SLT-GRPO on the CSL-Daily dataset. The baseline corresponds to the SLT-SFT model. The performance shown in the SLT-GRPO curve reflects results on the validation set of CSL-Daily.

**Ablation on the reward functions.** We conduct experiments using different reward functions. As shown in Table 7, using either BLEU or ROUGE alone already yields competitive performance, while combining the two leads to further improvements. This indicates that, under the sentence-level reinforcement optimization strategy, jointly using BLEU and ROUGE as rewards effectively constrains both the fidelity and completeness of the generated sentences, ultimately resulting in better translation quality.

#### 4.4. Analysis

**Reward Learning Curve.** We evaluate the checkpoints of the RFT stage every 100 steps to plot the learning curve, as shown in Fig. 3. The SLT-GRPO model consistently outperforms SLT-SFT across all checkpoints, showing continuous performance growth from 0 up to approximately 4500 training steps.

**Case Study.** We visualize the translation outputs of our method and C<sup>2</sup>RL on three randomly selected CSL-Daily samples. As shown in Table 8, both models generate reasonable translations, yet C<sup>2</sup>RL shows clear errors and omissions. Our method achieves higher lexical overlap and closer semantic alignment with the references, resulting in more accurate sentence-level correspondence. Even when wording differs, the intended meanings remain consistent. These findings indicate that richer sign representations allow the LLM to capture finer semantic cues, while GRPO-based optimization further improves translation fidelity and

Source	Sentence	Metrics
Reference	世界上没有后悔药 (There is no medicine for regret in the world.)	
C <sup>2</sup> RL	世界上没有 不 后悔 的作弊 There is no such thing as cheating without regret.	B-4: 40.35 R-L: 70.27
Ours	世界上没有后悔药 There is no medicine for regret in the world.	B-4: 100.00 R-L: 100.00
Reference	不要在家里看电视, 出去踢足球 (Don't stay home watching TV, go out and play football.)	
C <sup>2</sup> RL	不要 在家看电视 不去了 出去 踢足球 Don't staying home and watching TV instead of playing football.	B-4: 40.39 R-L: 76.03
Ours	不要在家里看电视, 去 踢足球 Don't stay home watching TV, go play football.	B-4: 78.82 R-L: 96.03
Reference	售货员在热情地向顾客介绍商品 (The salesperson is enthusiastically introducing the products to the customer.)	
C <sup>2</sup> RL	服务员不以冷淡的态度对待向 顾客 提供 商品 Waiters should not treat customers with indifference when serving goods.	B-4: 0.00 R-L: 30.47
Ours	商品员 在热情地向顾客介绍商品 The sales clerk enthusiastically introduced the products to the customer.	B-4: 69.81 R-L: 81.26

Table 8. Qualitative and quantitative comparison between C<sup>2</sup>RL and our method on the CSL-Daily dataset. English translations are obtained via Google Translate. Text segments highlighted in green denote exact matches with the reference, yellow indicates semantically similar expressions, purple marks omissions, and red denotes incorrect meanings. B-4: BLEU-4, R-L: ROUGE-L

completeness. Additional examples are included in the supplementary material.

#### 5. Conclusion

This paper presents RVLF, a unified three-stage framework for sign language translation that integrates cross-lingual visual-language pre-training, instruction-tuned fine-tuning, and GRPO-based reinforcement optimization. The proposed approach enhances sign representations and aligns sentence-level semantics, resulting in significant improvements in translation fidelity and completeness. Experiments on multiple benchmark datasets show that RVLF achieves state-of-the-art performance, surpassing even models pre-trained on large-scale external sign language corpora.

**Limitations and Future Work.** RVLF performs well without external pre-training, but its results are limited by the size and diversity of current benchmarks. Due to computational constraints, LoRA was used during LLM fine-tuning, and the model’s full potential remains unexplored. Future work will focus on scaling the framework with larger, real-world sign language datasets.

## References

- [1] Rafael V Azevedo, Thiago M Coutinho, Joao P Ferreira, Thiago L Gomes, and Erickson R Nascimento. Empowering sign language communication: Integrating sentiment and semantics for facial expression synthesis. *Computers & Graphics*, 124:104065, 2024. 1
- [2] Shuai Bai, Keqin Chen, Xuejing Liu, Jialin Wang, Wenbin Ge, Sibao Song, Kai Dang, Peng Wang, Shijie Wang, Jun Tang, et al. Qwen2. 5-vl technical report. *arXiv preprint arXiv:2502.13923*, 2025. 3
- [3] Necati Cihan Camgoz, Simon Hadfield, Oscar Koller, Hermann Ney, and Richard Bowden. Neural sign language translation. In *Proceedings of the IEEE conference on computer vision and pattern recognition*, pages 7784–7793, 2018. 2, 6, 7
- [4] Necati Cihan Camgoz, Simon Hadfield, Oscar Koller, Hermann Ney, and Richard Bowden. Neural sign language translation. In *Proceedings of the IEEE conference on computer vision and pattern recognition*, pages 7784–7793, 2018. 1, 5
- [5] Necati Cihan Camgoz, Oscar Koller, Simon Hadfield, and Richard Bowden. Sign language transformers: Joint end-to-end sign language recognition and translation. In *Proceedings of the IEEE/CVF conference on computer vision and pattern recognition*, pages 10023–10033, 2020. 1, 2, 6
- [6] Yutong Chen, Fangyun Wei, Xiao Sun, Zhirong Wu, and Stephen Lin. A simple multi-modality transfer learning baseline for sign language translation. In *Proceedings of the IEEE/CVF conference on computer vision and pattern recognition*, pages 5120–5130, 2022. 6
- [7] Yutong Chen, Ronglai Zuo, Fangyun Wei, Yu Wu, Shujie Liu, and Brian Mak. Two-stream network for sign language recognition and translation. *Advances in Neural Information Processing Systems*, 35:17043–17056, 2022. 1, 2, 6
- [8] Zhigang Chen, Benjia Zhou, Jun Li, Jun Wan, Zhen Lei, Ning Jiang, Quan Lu, and Guoqing Zhao. Factorized learning assisted with large language model for gloss-free sign language translation. In *Proceedings of the 2024 Joint International Conference on Computational Linguistics, Language Resources and Evaluation (LREC-COLING 2024)*, pages 7071–7081, 2024. 1, 3, 6, 7
- [9] Zhigang Chen, Benjia Zhou, Yiqing Huang, Jun Wan, Yibo Hu, Hailin Shi, Yanyan Liang, Zhen Lei, and Du Zhang. C 2 rl: Content and context representation learning for gloss-free sign language translation and retrieval. *IEEE Transactions on Circuits and Systems for Video Technology*, 2025. 1, 2, 3, 6, 7
- [10] Yiting Cheng, Fangyun Wei, Jianmin Bao, Dong Chen, and Wenqiang Zhang. Cico: Domain-aware sign language retrieval via cross-lingual contrastive learning. In *Proceedings of the IEEE/CVF Conference on Computer Vision and Pattern Recognition*, pages 19016–19026, 2023. 3
- [11] Zesen Cheng, Sicong Leng, Hang Zhang, Yifei Xin, Xin Li, Guanzheng Chen, Yongxin Zhu, Wenqi Zhang, Ziyang Luo, Deli Zhao, and Lidong Bing. Videollama 2: Advancing spatial-temporal modeling and audio understanding in video-llms. *arXiv preprint arXiv:2406.07476*, 2024. 2, 5
- [12] Phoebe Chua, Cathy Mengying Fang, Yasith Samaradiyakara, Pattie Maes, and Suranga Nanayakkara. Perspectives on capturing emotional expressiveness in sign language. *arXiv preprint arXiv:2505.08072*, 2025. 1
- [13] MMPose Contributors. Openmmlab pose estimation toolbox and benchmark. <https://github.com/open-mmlab/mmpose>, 2020. 3
- [14] Amanda Duarte, Shruti Palaskar, Lucas Ventura, Deepti Ghadiyaram, Kenneth DeHaan, Florian Metzke, Jordi Torres, and Xavier Giro-i Nieto. How2sign: a large-scale multimodal dataset for continuous american sign language. In *Proceedings of the IEEE/CVF conference on computer vision and pattern recognition*, pages 2735–2744, 2021. 5
- [15] Shiwei Gan, Yafeng Yin, Zhiwei Jiang, Lei Xie, and Sanglu Lu. Towards real-time sign language recognition and translation on edge devices. In *Proceedings of the 31st ACM International Conference on Multimedia*, pages 4502–4512, 2023. 1, 2
- [16] Jia Gong, Lin Geng Foo, Yixuan He, Hossein Rahmani, and Jun Liu. Llms are good sign language translators. In *Proceedings of the IEEE/CVF Conference on Computer Vision and Pattern Recognition*, pages 18362–18372, 2024. 1, 3, 6
- [17] Shester Gueuwou, Xiaodan Du, Greg Shakhnarovich, and Karen Livescu. Signmusketeers: An efficient multi-stream approach for sign language translation at scale. In *Findings of the Association for Computational Linguistics: ACL 2025*, pages 22506–22521, 2025. 1, 2, 7
- [18] Daya Guo, Dejian Yang, Haowei Zhang, Junxiao Song, Peiyi Wang, Qihao Zhu, Runxin Xu, Ruoyu Zhang, Shirong Ma, Xiao Bi, et al. Deepseek-r1 incentivizes reasoning in llms through reinforcement learning. *Nature*, 645(8081):633–638, 2025. 3
- [19] Wenxuan Huang, Bohan Jia, Zijie Zhai, Shaosheng Cao, Zheyu Ye, Fei Zhao, Zhe Xu, Yao Hu, and Shaohui Lin. Vision-r1: Incentivizing reasoning capability in multimodal large language models. *arXiv preprint arXiv:2503.06749*, 2025. 3
- [20] Aaron Jaech, Adam Kalai, Adam Lerer, Adam Richardson, Ahmed El-Kishky, Aiden Low, Alec Helyar, Aleksander Madry, Alex Beutel, Alex Carney, et al. Openai o1 system card. *arXiv preprint arXiv:2412.16720*, 2024. 3
- [21] Peiqi Jiao, Yuecong Min, Yanan Li, Xiaotao Wang, Lei Lei, and Xilin Chen. Cosign: Exploring co-occurrence signals in skeleton-based continuous sign language recognition. In *Proceedings of the IEEE/CVF international conference on computer vision*, pages 20676–20686, 2023. 3, 6, 1
- [22] Peiqi Jiao, Yuecong Min, and Xilin Chen. Visual alignment pre-training for sign language translation. In *European Conference on Computer Vision*, pages 349–367. Springer, 2024. 1, 3, 6, 7
- [23] Dongxu Li, Chenchen Xu, Xin Yu, Kaihao Zhang, Benjamin Swift, Hanna Suominen, and Hongdong Li. Tspnet: Hierarchical feature learning via temporal semantic pyramid for sign language translation. *Advances in Neural Information Processing Systems*, 33:12034–12045, 2020. 2, 6

- [24] Zecheng Li, Wengang Zhou, Weichao Zhao, Kepeng Wu, Hezhen Hu, and Houqiang Li. Uni-sign: Toward unified sign language understanding at scale. In *The Thirteenth International Conference on Learning Representations*, 2025. 1, 2, 3, 6, 7
- [25] Han Liang, Chengyu Huang, Yuecheng Xu, Cheng Tang, Weicai Ye, Juzhe Zhang, Xin Chen, Jingyi Yu, and Lan Xu. Llava-slt: Visual language tuning for sign language translation. *arXiv preprint arXiv:2412.16524*, 2024. 6
- [26] Chin-Yew Lin. Rouge: A package for automatic evaluation of summaries. In *Text summarization branches out*, pages 74–81, 2004. 5
- [27] Kezhou Lin, Xiaohan Wang, Linchao Zhu, Ke Sun, Bang Zhang, and Yi Yang. Gloss-free end-to-end sign language translation. *arXiv preprint arXiv:2305.12876*, 2023. 7
- [28] Haotian Liu, Chunyuan Li, Qingyang Wu, and Yong Jae Lee. Visual instruction tuning. *Advances in neural information processing systems*, 36:34892–34916, 2023. 2, 3, 6
- [29] Haotian Liu, Chunyuan Li, Yuheng Li, Bo Li, Yuanhan Zhang, Sheng Shen, and Yong Jae Lee. Llavavnext: Improved reasoning, ocr, and world knowledge, 2024. 2
- [30] Yinhan Liu, Jiatao Gu, Naman Goyal, Xian Li, Sergey Edunov, Marjan Ghazvininejad, Mike Lewis, and Luke Zettlemoyer. Multilingual denoising pre-training for neural machine translation. *Transactions of the Association for Computational Linguistics*, 8:726–742, 2020. 3
- [31] Ilya Loshchilov and Frank Hutter. Decoupled weight decay regularization. *arXiv preprint arXiv:1711.05101*, 2017. 6
- [32] Maxime Oquab, Timothée Darcet, Théo Moutakanni, Huy Vo, Marc Szafraniec, Vasil Khalidov, Pierre Fernandez, Daniel Haziza, Francisco Massa, Alaaeldin El-Nouby, et al. Dinov2: Learning robust visual features without supervision. *arXiv preprint arXiv:2304.07193*, 2023. 2, 3, 4, 5
- [33] Kishore Papineni, Salim Roukos, Todd Ward, and Wei-Jing Zhu. Bleu: a method for automatic evaluation of machine translation. In *Proceedings of the 40th annual meeting of the Association for Computational Linguistics*, pages 311–318, 2002. 5
- [34] Qwen Team. Qwen3-vl: Large vision-language model by alibaba cloud. <https://github.com/QwenLM/Qwen3-VL>, 2025. Accessed: 2025-11-04. 3
- [35] Alec Radford, Jong Wook Kim, Chris Hallacy, Aditya Ramesh, Gabriel Goh, Sandhini Agarwal, Girish Sastry, Amanda Askell, Pamela Mishkin, Jack Clark, et al. Learning transferable visual models from natural language supervision. In *International conference on machine learning*, pages 8748–8763. PmLR, 2021. 3
- [36] Herbert Robbins and Sutton Monro. A stochastic approximation method. *The annals of mathematical statistics*, pages 400–407, 1951. 6
- [37] Phillip Rust, Bowen Shi, Skyler Wang, Necati Cihan Camgöz, and Jean Maillard. Towards privacy-aware sign language translation at scale. *arXiv preprint arXiv:2402.09611*, 2024. 3, 7
- [38] Zhihong Shao, Peiyi Wang, Qihao Zhu, Runxin Xu, Junxiao Song, Xiao Bi, Haowei Zhang, Mingchuan Zhang, YK Li, Yang Wu, et al. Deepseekmath: Pushing the limits of mathematical reasoning in open language models. *arXiv preprint arXiv:2402.03300*, 2024. 2, 3
- [39] Bowen Shi, Diane Brentari, Gregory Shakhnarovich, and Karen Livescu. Open-domain sign language translation learned from online video. In *Proceedings of the 2022 Conference on Empirical Methods in Natural Language Processing*, pages 6365–6379, 2022. 5, 7
- [40] Laia Tarrés, Gerard I Gállego, Amanda Duarte, Jordi Torres, and Xavier Giró-i Nieto. Sign language translation from instructional videos. In *Proceedings of the IEEE/CVF Conference on Computer Vision and Pattern Recognition*, pages 5625–5635, 2023. 7
- [41] Marshall Thomas, Edward Fish, and Richard Bowden. Multistream-llm: Bridging modalities for robust sign language translation. *arXiv preprint arXiv:2509.00030*, 2025. 1
- [42] Dave Uthus, Garrett Tanzer, and Manfred Georg. Youtube-asl: A large-scale, open-domain american sign language-english parallel corpus. *Advances in Neural Information Processing Systems*, 36:29029–29047, 2023. 3, 7
- [43] Jun Wan, Qiuqi Ruan, Wei Li, and Shuang Deng. One-shot learning gesture recognition from rgb-d data using bag of features. *The Journal of Machine Learning Research*, 14(1): 2549–2582, 2013. 1
- [44] Jun Wan, Guodong Guo, and Stan Z Li. Explore efficient local features from rgb-d data for one-shot learning gesture recognition. *IEEE transactions on pattern analysis and machine intelligence*, 38(8):1626–1639, 2015. 1
- [45] Ryan Wong, Necati Cihan Camgoz, and Richard Bowden. Sign2GPT: Leveraging large language models for gloss-free sign language translation. In *The Twelfth International Conference on Learning Representations*, 2024. 1, 3, 6
- [46] An Yang, Anfeng Li, Baosong Yang, Beichen Zhang, Binyuan Hui, Bo Zheng, Bowen Yu, Chang Gao, Chengen Huang, Chenxu Lv, et al. Qwen3 technical report. *arXiv preprint arXiv:2505.09388*, 2025. 5
- [47] Yi Yang, Xiaoxuan He, Hongkun Pan, Xiyan Jiang, Yan Deng, Xingtao Yang, Haoyu Lu, Dacheng Yin, Fengyun Rao, Minfeng Zhu, et al. R1-onevision: Advancing generalized multimodal reasoning through cross-modal formalization. *arXiv preprint arXiv:2503.10615*, 2025. 3
- [48] Aoxiong Yin, Tianyun Zhong, Li Tang, Weike Jin, Tao Jin, and Zhou Zhao. Gloss attention for gloss-free sign language translation. In *Proceedings of the IEEE/CVF conference on computer vision and pattern recognition*, pages 2551–2562, 2023. 1, 2, 6
- [49] Jiahui Yu, Zirui Wang, Vijay Vasudevan, Legg Yeung, Mojtaba Seyedhosseini, and Yonghui Wu. Coca: Contrastive captioners are image-text foundation models. *arXiv preprint arXiv:2205.01917*, 2022. 4
- [50] Biao Zhang, Mathias Müller, and Rico Sennrich. Sltunet: A simple unified model for sign language translation. *arXiv preprint arXiv:2305.01778*, 2023. 6
- [51] Boqiang Zhang, Kehan Li, Zesen Cheng, Zhiqiang Hu, Yuqian Yuan, Guanzheng Chen, Sicong Leng, Yuming Jiang, Hang Zhang, Xin Li, et al. Videollama 3: Frontier multi-

- modal foundation models for image and video understanding. *arXiv preprint arXiv:2501.13106*, 2025. 2
- [52] Jian Zhao, Weizhen Qi, Wengang Zhou, Nan Duan, Ming Zhou, and Houqiang Li. Conditional sentence generation and cross-modal reranking for sign language translation. *IEEE Transactions on Multimedia*, 24:2662–2672, 2021. 2, 6
- [53] Rui Zhao, Liang Zhang, Biao Fu, Cong Hu, Jinsong Su, and Yidong Chen. Conditional variational autoencoder for sign language translation with cross-modal alignment. In *Proceedings of the AAAI Conference on Artificial Intelligence*, pages 19643–19651, 2024. 6
- [54] Benjia Zhou, Zhigang Chen, Albert Clapés, Jun Wan, Yanyan Liang, Sergio Escalera, Zhen Lei, and Du Zhang. Gloss-free sign language translation: Improving from visual-language pretraining. In *Proceedings of the IEEE/CVF International Conference on Computer Vision*, pages 20871–20881, 2023. 1, 2, 6, 3
- [55] Benjia Zhou, Pichao Wang, Jun Wan, Yanyan Liang, and Fan Wang. A unified multimodal de-and re-coupling framework for rgb-d motion recognition. *IEEE Transactions on Pattern Analysis and Machine Intelligence*, 45(10):11428–11442, 2023. 1
- [56] Hao Zhou, Wengang Zhou, Yun Zhou, and Houqiang Li. Spatial-temporal multi-cue network for continuous sign language recognition. In *Proceedings of the AAAI conference on artificial intelligence*, pages 13009–13016, 2020. 1, 2
- [57] Hao Zhou, Wengang Zhou, Weizhen Qi, Junfu Pu, and Houqiang Li. Improving sign language translation with monolingual data by sign back-translation. In *Proceedings of the IEEE/CVF conference on computer vision and pattern recognition*, pages 1316–1325, 2021. 1, 2, 5, 6
- [58] Hengguang Zhou, Xirui Li, Ruochen Wang, Minhao Cheng, Tianyi Zhou, and Cho-Jui Hsieh. R1-zero’s” aha moment” in visual reasoning on a 2b non-sft model. *arXiv preprint arXiv:2503.05132*, 2025. 3

# RVLF: A Reinforcing Vision–Language Framework for Gloss-Free Sign Language Translation

## Supplementary Material

To enable a thorough understanding of RVLF, this supplementary material presents more implementation details, further analyses, and more case studies. The core implementation code will be provided in the Supplementary Materials submitted alongside this file.

### 6. More Implementation Details

#### 6.1. Keypoints extraction.

We follow the keypoint extraction strategy in Cosign [21] and use the off-the-shelf estimator MMPose to obtain full-body keypoints from each frame of the sign-language videos. We select keypoints related to sign representation, including 9 body points, 21 points for each hand, 8 mouth points, and 18 facial points, giving a total of 77 keypoints. More details can be found in the Cosign [21].

#### 6.2. DINOv2 Feature extraction.

We first use full-body keypoints to detect the bounding boxes of the hands and face, then crop these regions and resize them to  $224 \times 224$ . If the detector fails to locate the hands or face in a given frame, we replace that frame with the most recent frame where detection succeeded. The cropped regions are then fed into a pre-trained DINOv2 model (facebook/dinov2-base) to extract semantically rich feature sequences.

#### 6.3. Training Setting.

In this section, we provide as many training details of RVLF as possible, including the computing infrastructure and the training configurations for each stage.

**Computing Infrastructure** The entire experimental process was conducted on a computational infrastructure comprising an Intel(R) Xeon(R) Gold 6226R CPU @ 2.90GHz, 4 Tesla V100S GPU with 32GB of VRAM, running the Ubuntu 20.04 operating system, with Python 3.10, CUDA 11.8, transformers 4.51.3 and PyTorch 2.1.2.

**Settings on Pre-training Stage** The settings for the pre-training stage are summarized in Table 9. This stage involves training for 200 epochs using the SGD optimizer with a learning rate of 0.01 and a weight decay of 0.001. A cosine learning rate scheduler is applied, with a warm-up period of 20 epochs, which corresponds to 10% of the total training epochs. The batch size is set to 8, and the cross-entropy loss is used as the training objective. In the

Training settings		Model settings	
Config	Value	Config	Value
epoch	200	MHA Number	8
Optimizer	SGD	Layer Number	3
Learning Rate	0.01	Hidden Size	512
Weight Decay	0.001	FF Dimension	2048
Scheduler	Cosine	Beam Search Width	5
Cycle Decay	1.0	Vocab Size	6201
Batch Size	8	Max Length	300
Criterion	CrossEntropy	Con Dimension	1024

Table 9. Settings for pre-training stage. FF Dimension : feed-forward dimension; Con Dimension : Contrastive Dimension.

Training settings		Model settings	
Config	Value	Config	Value
Epoch	40	Projector Modules	mlp + gelu
Batch Size	4	MLP Dim	512,4096,4096
Optimizer	AdamW	LLM	Qwen3-8B
LR	$2 \times 10^{-4}$	Target Modules	q-proj, v-proj
Projector LR	$2 \times 10^{-5}$	Rank	16
Weight Decay	0	Scaling Factor	32
Scheduler	Cosine	LoRA Dropout	0.3
Cycle Decay	1.0	Max Length	300
Criterion	CrossEntropy	Beam Search Width	5

Table 10. Settings for supervised fine-tuning stage. LR : Learning Rate; q-proj : query projection matrices; v-proj : value projection matrices.

pre-training stage, both the text encoder and decoder are built by reinitializing the first three layers of the mBART model. In contrast, the skeleton encoder is implemented as a mBART encoder with three layers. The text encoder, decoder, and skeleton encoder all follow the same configuration, where each Transformer block consists of an 8-head multi-head self-attention mechanism, a hidden size of 512, and a feed-forward network with a dimensionality of 2048. Following [54], we reduce the original vocabulary to a task-specific subset, resulting in a final vocabulary size of 6,201 (for CSL-Daily Dataset). The maximum input sequence length is limited to 300, as explained in Section 7.1. For contrastive learning, we fix the feature dimension of both vision and text inputs to 1024. During text decoding, we use a beam width of 5.

**Settings on Supervised Fine-Tuning Stage** The training settings for the supervised fine-tuning stage are shown in Table 10. The model is trained for 40 epochs using the AdamW optimizer. The LLM parameters use a learning rate of  $2 \times 10^{-4}$ , while the multimodal projector uses a learning rate of  $2 \times 10^{-5}$ . Weight decay is set to 0. A cosine learning rate schedule with 8 warmup epochs is ap-

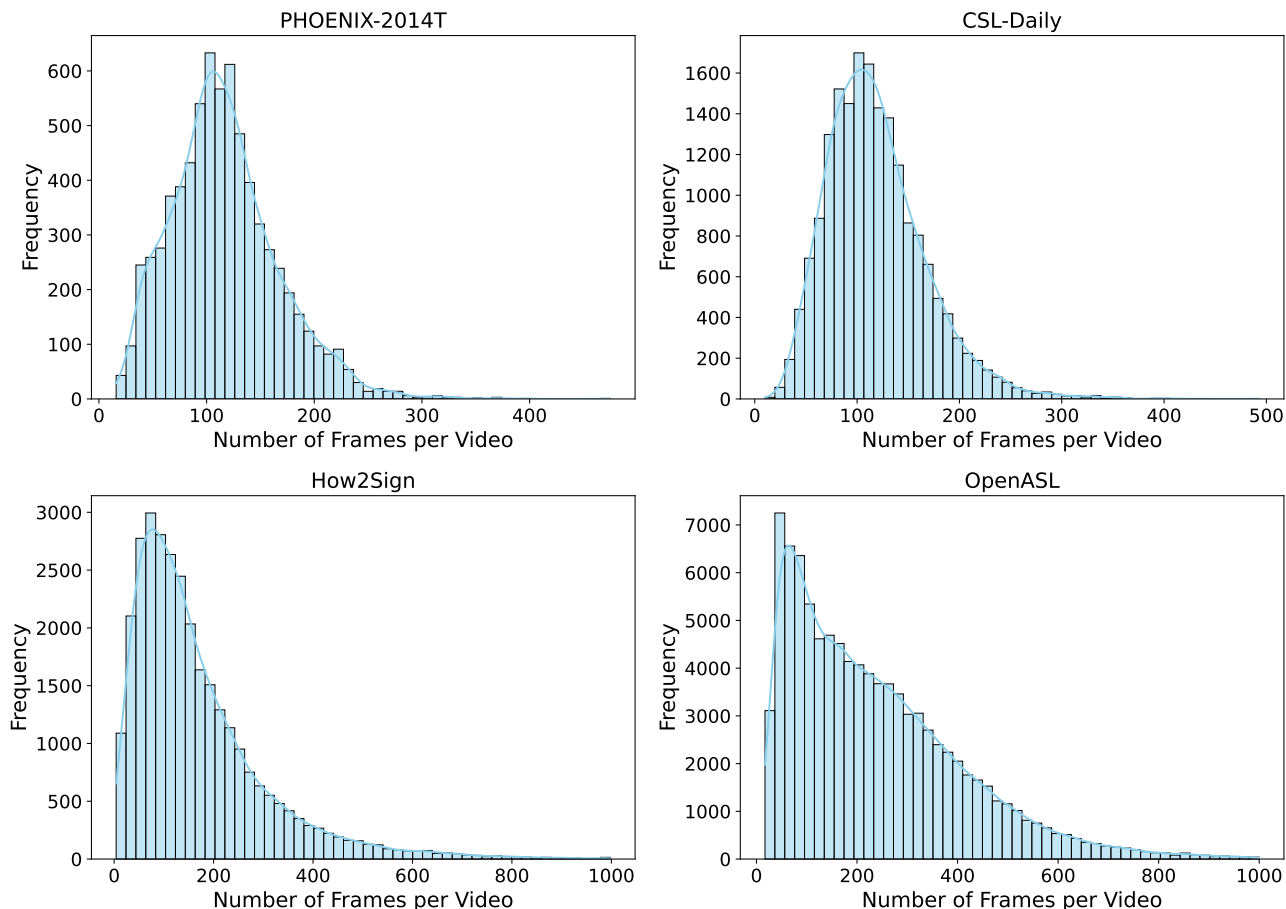


Figure 4. Visualization of the input length distribution of sign language videos in the training sets of four datasets: PHOENIX-2014T, CSL-Daily, PHOENIX-2014T How2Sign, and OpenASL. Due to the significant long-tail phenomenon in the frame count distributions of How2Sign and OpenASL, only samples with a frame count of 1000 or fewer are included in the visualization to improve readability, while still covering the vast majority of samples in both datasets.

Training settings		Model settings	
Config	Value	Config	Value
Epoch	2	LLM	Qwen3-8B
Batch Size	8	Target Modules	q-proj, v-proj
Optimizer	AdamW	Rank	64
LR	$2 \times 10^{-5}$	Scaling Factor	128
Responses	8	LoRA Dropout	0.05
Weight Decay	0	Max Length	300
Criterion	BELU & ROUGE	Beam Search Width	5

Table 11. Settings for reinforcement fine-tuning stage.

plied. The batch size is 4, and cross-entropy loss is used as the training objective. Following LLaVA [28], we adopt a two-layer MLP projector with GELU activation, which expands the 512-dimensional visual feature to 4096 dimensions and applies another 4096-dimensional linear layer to produce visual embeddings compatible with the language model. Qwen3-8B serves as the base language model. To

enable parameter-efficient training, we apply LoRA to the query and value projection matrices in the self-attention layers, using rank 16, a scaling factor of 32, and a dropout rate of 0.3. The instruction template is set as: “A conversation between a deaf person and an AI assistant. The assistant can generate accurate and fluent translated text based on provided sign language visual information.” The maximum input sequence length is 300, and the motivation is discussed in Sec. 7.1. During inference, we use deterministic beam search with a beam width of 5 and disable sampling.

**Settings on Reinforcement Fine-Tuning Stage** After merging the LoRA parameters from the SFT stage into the base model, we obtain the SLT-SFT model. The training settings for the reinforcement fine-tuning stage are summarized in Table 11. In this stage, we add new LoRA mod-

Frame Length	PHOENIX14T	CSL-Daily	How2Sign	OpenASL
>300	23	90	4338	29172
>500	0	0	1180	8226
>800	0	0	258	1138
>1000	0	0	140	362
Total Samples	7096	18401	31064	95888

Table 12. Comparison of training samples exceeding different frame-length thresholds across four large-scale sign language datasets: PHOENIX14T, CSL-Daily, How2Sign, and OpenASL.

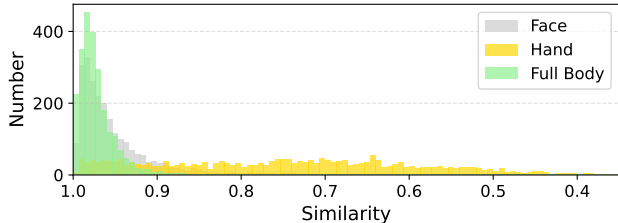


Figure 5. Stacked histogram of frame-to-frame similarity for full body, face, and hand regions.

ules to the query and value projection matrices in the self-attention layers, using rank 64, a scaling factor of 128, and a dropout rate of 0.05. We use the AdamW optimizer with a learning rate of  $2 \times 10^{-5}$ , train for two epochs, and use a batch size of 8. Following the [38] setting and using the same prompts as in the SFT stage, we sample 8 candidate responses for each input. These responses are grouped to compute relative rewards based on BLEU-4 and ROUGE-L and to estimate advantages for policy updates. As in the SFT stage, the maximum input sequence length is set to 300. During inference, we use beam search with a beam width of 5. A practical detail is that some sign language datasets contain very short sentences. To reduce unstable BLEU-4 scores that may interrupt training, we append additional punctuation to the end of these sentences.

## 7. Further Analyses

### 7.1. Dataset Input Sequence Length Analysis

The sign language datasets exhibit substantial variation in sequence length. As shown in Figures 4 and Table 12, How2Sign and OpenASL contain a markedly higher proportion of long sequences than PHOENIX14T and CSL-Daily, reflecting greater linguistic complexity. Due to GPU memory limits and heterogeneous length distributions, all sequences are truncated to 300 frames during training. In contrast, the VAP paper employs NVIDIA RTX A800 GPUs, which likely support longer sequences and require less truncation. This difference may partially explain the larger performance gains reported on their benchmarks relative to the more modest improvements observed on How2Sign and OpenASL. The limited improvement on PHOENIX14T is more plausibly due to the already strong performance of existing methods on this dataset and the

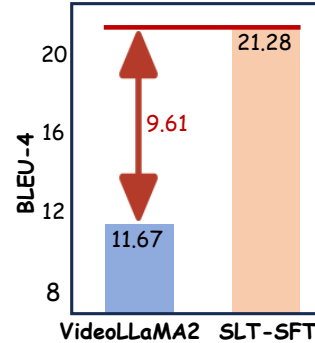


Figure 6. Performance comparison between directly fine-tuning VideoLLaMA2 and the SLT-SFT model.

comparatively smaller amount of German-language training data available in Qwen3.

### 7.2. Effect of Visual Representations.

**Visual Region** The analysis of frame-to-frame cosine similarity for full-body, face, and hand features reveals clear temporal differences. Cosine similarity is computed between adjacent frames, and the distribution is shown in Figure 5. Hand and face features show greater variation compared to full-body features, indicating that they contain rich temporal cues that are crucial for modeling sign transitions. Full-body features, on the other hand, remain relatively stable because static regions and background elements dominate the representation. These findings suggest that the hand and face regions provide more informative and discriminative visual signals, which are essential for temporal modeling in sign language understanding.

**Visual Encoder** To investigate the capabilities of different pretrained visual encoders on the SLT task, we examine the feature distributions output by various visual encoder backbones. Specifically, we compute the inter-frame cosine similarity of face and hand region features output by different encoders (i.e., DINOv2 and ResNet-18). For the ResNet-18 baseline, we follow [54] and employ a ResNet model pretrained on ImageNet. As shown in Fig. 7, features extracted by ResNet-18 exhibit high redundancy, with similarity scores densely concentrated around 1.0, indicating its inability to capture subtle yet crucial temporal variations in sign language. By contrast, DINOv2 yields a broader and more diverse similarity distribution, particularly for hand features, indicating that DINOv2 can provide informative sign representations thanks to its strong vision perception.

### 7.3. Directly Fine-Tuning a Video LLM

Collecting large-scale sign language datasets is difficult because annotation is expensive and skilled signers are limited. This leads to a clear gap between visual and textual

Source	Sentence	Objective Metrics
<b>Reference</b>	liebe zuschauer guten abend ( <i>Dear viewers, good evening</i> )	
<b>C<sup>2</sup>RL</b>	liebe zuschauer guten abend ( <i>Dear viewers, good evening</i> )	BLEU-4: 0.00 ROUGE.L: 67.11
<b>Ours</b>	liebe zuschauer guten abend ( <i>Dear viewers, good evening</i> )	BLEU-4: 100.00 ROUGE.L: 100.00
<b>Reference</b>	am sonntag ziehen von nordwesten wieder schauer und gewitter heran ( <i>On Sunday, showers and thunderstorms will approach again from the northwest</i> )	
<b>C<sup>2</sup>RL</b>	am sonntag breiten sich von westen wieder schauer und gewitter aus heran ( <i>On Sunday, showers and thunderstorms will spread from the west</i> )	BLEU-4: 0.00 ROUGE.L: 63.64
<b>Ours</b>	am sonntag ziehen dann von nordwesten schauer und gewittern heran ( <i>On Sunday, showers and thunderstorms will then approach from the northwest</i> )	BLEU-4: 51.57 ROUGE.L: 90.91
<b>Reference</b>	in der nacht muss vor allem in der nordwesthälfte mit schauern und gewittern gerechnet werden die heftig ausfallen können ( <i>During the night, showers and thunderstorms are to be expected, especially in the northwestern half, which can be severe</i> )	
<b>C<sup>2</sup>RL</b>	in der nacht muss vor allem im nordwesten mit einzelnen schauern und gewittern gerechnet werden die mitunter kräftig sein können ( <i>During the night, isolated showers and thunderstorms are to be expected, especially in the northwest, which can be severe</i> )	BLEU-4: 48.46 ROUGE.L: 73.08
<b>Ours</b>	in der nacht muss vor allem in der nordwesthälfte mit schauern und gewittern gerechnet werden die mitunter kräftig ausfallen können ( <i>During the night, showers and thunderstorms are to be expected, especially in the northwestern half, which can sometimes be heavy</i> )	BLEU-4: 81.37 ROUGE.L: 92.57

Table 13. Qualitative and quantitative comparison between C<sup>2</sup>RL and our method on the **PHOENIX14T** dataset. English translations are obtained via *Google Translate*. Text segments highlighted in green denote exact matches with the reference, yellow indicates semantically similar expressions, purple marks omissions, and red denotes incorrect meanings.

Source	Sentence	Objective Metrics
<b>Reference</b>	i'm here telling you how to wash your jeans	
<b>C<sup>2</sup>RL</b>	i'm here to talk to you about how to wash your clothes	BLEU-4: 26.20 ROUGE.L: 64.10
<b>Ours</b>	i'm here to tell you how to wash your jeans	BLEU-4: 58.14 ROUGE.L: 83.75
<b>Reference</b>	you can take this forward and back, you can take it in a circle, you can take it in a lot of different directions.	
<b>C<sup>2</sup>RL</b>	you can put it on the floor, you can put it around the house, you can do different things	BLEU-4: 0.00 ROUGE.L: 36.24
<b>Ours</b>	you can take this forward and back, you can take it sideways, you can take it in a lot of different directions.	BLEU-4: 79.67 ROUGE.L: 90.96
<b>Reference</b>	so, i'm going to turn on my sequencer and i'm just going to press play and you can just go to each one and just hear a different presets	
<b>C<sup>2</sup>RL</b>	i'm hooping, my note cards, i'm going to these players as fast as you can, and you're just going to follow one and hear the difference between the note cards	BLEU-4: 0.00 ROUGE.L: 36.24
<b>Ours</b>	so i changed my settings and i'm just going to press play and you can just go to each one and hear the different presets	BLEU-4: 79.67 ROUGE.L: 90.96

Table 14. Qualitative and quantitative comparison between C<sup>2</sup>RL and our method on the **How2Sign** dataset. Text segments highlighted in green denote exact matches with the reference, yellow indicates semantically similar expressions, purple marks omissions, and red denotes incorrect meanings.

Source	Sentence	Objective Metrics
Reference	Port Authority said the girl was playing with her grandfather in a dining hall	
C <sup>2</sup> RL	Grant's authorities said he is a girl and that he plays with his grandfather at a nursing home	BLEU-4: 0.00 ROUGE.L: 30.32
Ours	The Port Authority said the girl was playing with her grandfather in the dining hall	BLEU-4: 74.87 ROUGE.L: 89.44
Reference	Bernie Sanders won big in Nevada's on Saturday with 47% of the popular vote	
C <sup>2</sup> RL	Bernie Sanders won the primaries in Nevada on Saturday and his popular caucuses on Saturday	BLEU-4: 0.00 ROUGE.L: 46.67
Ours	Bernie Sanders won big in Nevada's caucuses on Saturday with 47% of the popular vote	BLEU-4: 72.98 ROUGE.L: 91.92
Reference	Thursday marks exactly six months since the World Health Organization declared Covid-19 a public health emergency	
C <sup>2</sup> RL	As of Thursday morning the World Health Organization (WHO) has been declared a "coronavirus crisis."	BLEU-4: 17.70 ROUGE.L: 45.07
Ours	Thursday marks exactly six months since the World Health Organization declared Covid-19 a public health emergency	BLEU-4: 84.15 ROUGE.L: 96.57

Table 15. Qualitative and quantitative comparison between C<sup>2</sup>RL and our method on the **OpenASL** dataset. Text segments highlighted in green denote exact matches with the reference, yellow indicates semantically similar expressions, purple marks omissions, and red denotes incorrect meanings.

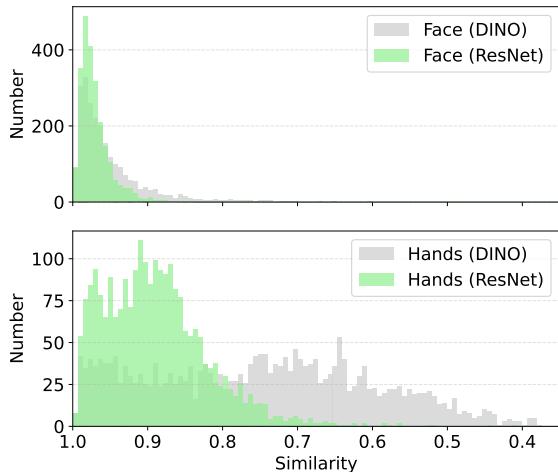


Figure 7. Analyzing the impact of vision distribution. Cosine similarity distribution map between adjacent frames of ResNet-18 and DINOv2. Twenty different samples were randomly selected from the CSL-Daily dataset.

modalities. Video LLMs provide strong temporal modeling and natural language generation abilities, which suggests that fine-tuning them with only a small number of sign-text pairs could support effective cross-modal alignment while reducing both data requirements and training cost. As a result, adapting powerful Video LLMs for sign language translation is a promising direction. To ensure a fair comparison and isolate the contribution of the model architecture, we strictly follow the official training configuration of VideoLLaMA2: all training settings and hyperparameters remain unchanged, and only the video data is re-

placed with sign-language datasets. However, as shown in Fig. 6, our earlier experiments reveal a large performance gap between directly fine-tuning VideoLLaMA2 (7B) [11] on sign-text pairs and the SLT-SFT model. A main reason is that sign language semantics are more structured and abstract than general video content, and the visual encoder of VideoLLaMA2 fails to learn discriminative sign representations. In addition, the linguistic granularity required for SLT is substantially higher than that for generic video understanding, making it difficult for a general-purpose video encoder to capture subtle phonological and morphological cues in sign videos. Although our analysis is based on a relatively simple experimental setting, exploring Video LLMs with stronger visual backbones and larger parameter scales remains a promising direction for future work.

## 8. More Case Studys

We conducted qualitative and quantitative analyses of the texts generated by RVLf and C<sup>2</sup>RL using translation samples from the PHOENIX14T, How2Sign, and OpenASL test sets, as shown in Tables 13, 14, and 15. The outputs from RVLf contain a larger number of words that match the ground-truth references, and their overall semantics are more consistent with the reference texts. This improvement is mainly due to the richer sign language representations produced by RVLf, which allow the model to capture semantic information more effectively. Additionally, RVLf benefits from a more robust feature extraction process, enabling it to better handle variations in sign language data. In addition, RVLf introduces a sentence-level reinforcement optimization strategy that helps maintain stronger semantic consistency and improves translation accuracy.